An attitude algorithm based on the band seamless splicing imaging for agile satellite*

WANG Ya-min (王亚敏)[1,2], **XU Wei** (徐伟)[1]**, **JIN Guang** (金光)[1], **YANG Xiu-bin** (杨秀彬)[1], and **ZHANG Zhao** (张钊)[1,2]

1. Changchun Institute of Optics, Fine Mechanics and Physics, Chinese Academy of Sciences, Changchun 130033, China

2. University of Chinese Academy of Sciences, Beijing 100049, China

(Received 15 March 2017; Revised 23 May 2017)

In order to realize fast maneuvering imaging of the target area with high resolution agile satellite, a new attitude matching algorithm is developed. A strict mosaic imaging model of ray trace and the velocity vector mapping are built according to the strip mosaic imaging principle and the relationship between imaging target and the camera focal plane. The three-axis attitude is deduced based on the principle of optimal tracking of the maneuvering path. Finally, the geometric scaling simulation is carried out through the time delayed and integration (TDI) charge coupled device (CCD) prototype system, satellite attitude control physical simulation platform and the LED earth target simulator. The experimental results show that the algorithm could realize the matching band seamless splicing imaging of the target very well, confirming the correctness of the algorithm.

Document code: A **Article ID:** 1673-1905(2017)05-0376-5

DOI https://doi.org/10.1007/s11801-017-7058-x

With the development of remote sensing, the imaging requirement of regional target is enhanced[1]. Since the area is larger and the shape is more irregular, traditional methods could not achieve a full coverage of the regional target in an orbit cycle when its width exceeds the satellite payload index. Modern agile satellite with integrated design has high imaging resolution, strong maneuverability and large imaging width so as to realize high resolution band splicing imaging rapidly[2]. During the process of band splicing imaging, the agile satellite needs to rapidly maneuver and maintain a specific attitude aligned with starting point of each band to perform matched push-broom imaging in different orbital positions. At present, a representative of band splicing imaging is the French Pleiades satellite. It adopts the way of making the whole satellite rotate around the roll axis and pitch axis so that the observation angle can be adjusted in a short time. When the roll angle is 30°, its maximum observation area can be up to 60 km (perpendicular to the track, three bands) × 315 km (along the track)[3].

There have been some researches on the band splicing imaging of agile satellite. Ref.[4] proposed one-orbit multi-stripes splicing imaging for agile satellite. In Ref.[5], the observed bands of the regional target were divided by the satellite field angle and the overlap rate. In Ref.[6], the foreground and the background pixels of two bands were respectively stitched and deformed after the band images transmitted to the ground. Ref.[7] discussed the attitude guidance technology for the cross-track acquisition of imaging mode of dynamic imaging mission. In the above reports, only preliminary analyses were carried out on the imaging of band splicing. They cannot solve the problem of satellite band splicing imaging systemically.

In this paper, a new attitude algorithm of band seamless splicing imaging is proposed. It solves the problem of uncertainty and mismatch between adjacent bands caused by the satellite large-angle maneuver and the earth curvature, according to the optimal maneuvering path and the matching relationship between the band velocity vector and imaging direction. Finally, the ground simulation is carried out to demonstrate the correctness of the algorithm. The computational process is simplified at the same time.

The design of the band seamless splicing imaging needs to establish the relationship between the ground target and the image plane. The rapid maneuver of satellite leads to the motion of satellite body coordinate system relative to the orbit coordinate and inertial coordinate[8]. The corresponding position vector and velocity vector are related in different three-dimensional coordinate systems. In order to facilitate subsequent mathematical modeling, it is necessary to define a reference coordinate system, as shown in Fig.1[9].

* This work has been supported by the Youth Innovation Promotion Association (No.2017261).

** E-mail: xwciomp@126.com

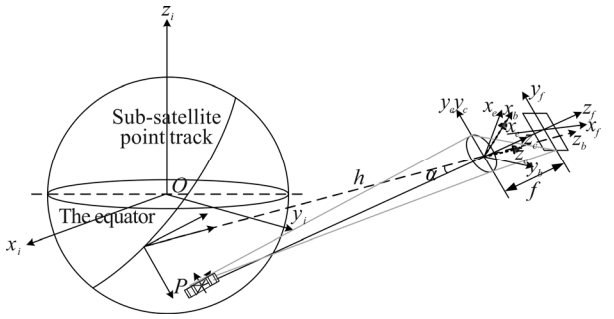

Fig.1 Reference coordinate system definition

In order to achieve the band splicing imaging, we need to determine the imaging sequence and mark off bands according to the satellite maneuver capability, camera width constraint, and band overlapping rate[10]. As shown in Fig.2, the satellite position is *S*, *H* is the orbit altitude, η is the view angle of the satellite, and the earth's radius is R_e. The view angle corresponding to the overlap region is $\eta_{overlap}$, whose value is constant all the time. *A*, *B* and *C* are the starting points of each band, respectively. Assuming that the latitude and longitude of *A* are (γ_A, λ_A) and its roll angle is φ_A, the roll angle of *B* can be obtained as[11]

$$\varphi_B = \varphi_A - \eta + \eta_{\text{overlap}} \quad . \tag{1}$$

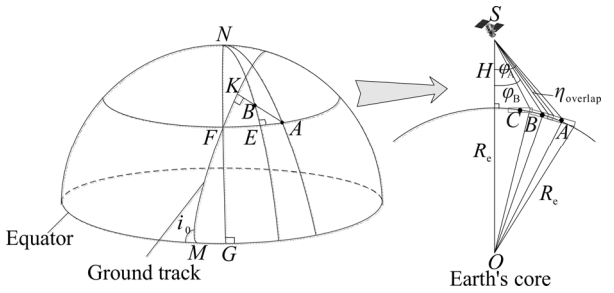

Fig.2 Geometric relationship of band splicing imaging

The orbit inclination is i_0. The ground track intersects the equator at *M*. *AB* is perpendicular to the ground track, whose pedal is *K*. Due to the geometrical relationship, ΔAKF is similar to ΔABE. In the same way, the exact location of the starting point *C* can be achieved. The bandwidth is the width of the satellite on the ground. Then we have

$$\begin{cases} \sin\widehat{AE} = \dfrac{\sin\angle ABE \sin\widehat{AB}}{\sin\angle AEB} \\ \tan\dfrac{\widehat{BE}}{2} = \dfrac{\cos\dfrac{\angle AEB+\angle ABE}{2}}{\cos\dfrac{\angle AEB-\angle ABE}{2}} \tan\dfrac{\widehat{AB}+\widehat{AE}}{2} \end{cases} , \tag{2}$$

$$\widehat{AB} = \pi - \varphi_A - \arcsin\left(\frac{H}{R_e}\sin\varphi_A\right) , \tag{3}$$

$$\begin{cases} \gamma_B = \gamma_A - \widehat{AE} \\ \lambda_B = \lambda_A + \widehat{BE} \cdot \end{cases} \tag{4}$$

The optical axis of the detector should be coincident with the observation vector, as shown in Fig.3. For most of the earth observation satellites, the Euler axis is perpendicular to the yaw axis. That is to say, the value of the yaw angle is not unique, while the other two have the only values regardless of the Euler rotation order.

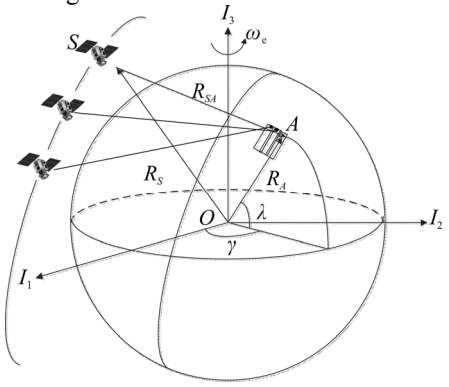

Fig.3 Schematic diagram of the band splicing imaging

Assuming that the coordinate of *A* in the geography coordinate system is (α_A, β_A, h_A), the position vector of *A* in the geocentric inertial coordinate system can be expressed as

$$\boldsymbol{R}'_A = \begin{bmatrix} x'_A \\ y'_A \\ z'_A \end{bmatrix} = |\boldsymbol{R}_A| \cdot \begin{bmatrix} \cos\beta\cos\alpha \\ \cos\beta\sin\alpha \\ \sin\beta \end{bmatrix} , \tag{5}$$

$$|\boldsymbol{R}_A| = \sqrt{\frac{a_e^2 \cdot b_e^2 \cdot (1+\tan^2\beta)}{b_e^2 + a_e^2 \cdot \tan^2\beta}} + h_A = \frac{a_e b_e}{\sqrt{a_e^2 \cdot \sin^2\beta + b_e^2 \cdot \cos^2\beta}} + h_A , \tag{6}$$

where $|\boldsymbol{R}_A|$ is the length of the vector from point *A* to the core of the earth, and a_e and b_e are the long half axis and the short half axis of earth, respectively. The observation vector $\boldsymbol{R}_{SA}^O$ in the orbit coordinate system can be described as

$$\boldsymbol{R}_{SA}^O = \boldsymbol{A}_I^O(\boldsymbol{R}_A^I - \boldsymbol{R}_S^I) = \boldsymbol{A}_I^O(\boldsymbol{A}_E^I \boldsymbol{R}_A^E - \boldsymbol{R}_S^I) , \tag{7}$$

$$\boldsymbol{A}_I^O = \boldsymbol{R}_{I_2}(-\pi/2)\boldsymbol{R}_{I_1}(-\pi/2)\boldsymbol{R}_{I_3}(u)\boldsymbol{R}_{I_1}(i_0)\boldsymbol{R}_{I_3}(\Omega) , \tag{8}$$

where $\boldsymbol{A}_i^o$ is the transformation matrix from the ground coordinate system to the orbit coordinate system, R_S^I is the position vector of satellite in geocentric inertial coordinate system, which can be given by the GPS, *u* is epoch angle, Ω is right ascension of ascending node, and $\boldsymbol{R}_{I_3}(\Omega)$ represents the coordinate transformation matrix around I_3 axis with a rotating angle Ω. The unit vector $\boldsymbol{u}_{SA}^O$ along the direction of observation vector in orbit coordinate system is

$$\boldsymbol{u}_{SA}^O = \frac{\boldsymbol{R}_{SA}^O}{|\boldsymbol{R}_{SA}^O|} , \tag{9}$$

and the satellite quaternion $\boldsymbol{Q}_A$ is

$$\boldsymbol{Q}_A = \left[\cos\frac{\vartheta}{2} \quad e\sin\frac{\vartheta}{2}\right]^{\mathrm{T}} = [q_{A0} \quad q_{A1} \quad q_{A2} \quad q_{A3}]^{\mathrm{T}} . \tag{10}$$

In order to make the optical axis u^O coincide with the observation vector $\boldsymbol{u}_{SA}^O$, the satellite has a number of maneuver paths. When the shortest path is selected, the expected four elements from the orbit coordinate system to the satellite body coordinate system can be expressed as

$$\vartheta = \arccos \frac{\boldsymbol{u}^O \cdot \boldsymbol{u}_{SA}^O}{\left|\boldsymbol{u}^O\right| \cdot \left|\boldsymbol{u}_{SA}^O\right|} , \tag{11}$$

$$\boldsymbol{e} = \frac{\boldsymbol{u}^O \times \boldsymbol{u}_{SA}^O}{\left|\boldsymbol{u}^O \times \boldsymbol{u}_{SA}^O\right|} , \tag{12}$$

where ϑ is the angle between the observation vector and the optical axis, $\boldsymbol{e}$ is a vertical unit vector to the observation vector and the optical axis, and q_{A0}, q_{A1}, q_{A2} and q_{A3} are the expected four elements.

When the 1-2-3 rotation is selected, the expected roll angle and the pitch angle in the satellite body coordinate system relative to the orbit coordinate system can be obtained as

$$\varphi_A = \arcsin\left[2(q_{A0}q_{A2} + q_{A1}q_{A3})\right] , \tag{13}$$

$$\theta_A = \arctan \frac{2(q_{A2}q_{A3} - q_{A0}q_{A1})}{q_{A0}^2 - q_{A1}^2 - q_{A2}^2 + q_{A3}^2} . \tag{14}$$

As shown in Fig.4, the ground resultant velocity is composed of two parts: a precession velocity caused by the orbital motion of the satellite and a velocity caused by the rotation of the earth. When the roll angle and pitch angle are known, the ground resultant velocity vector of the starting point can be confirmed as

$$\boldsymbol{V}_t = \boldsymbol{V}_s + \boldsymbol{V}_e, \boldsymbol{V}_s = \tau \cdot \left[\boldsymbol{R}_e - \boldsymbol{L}_A \cdot \cos\varphi_A\right] , \tag{15}$$

$$\boldsymbol{V}_e = \omega_e \cdot \boldsymbol{R}_e \cdot \cos\lambda_A , \tag{16}$$

$$\boldsymbol{L}_A = \left(\boldsymbol{H} + \boldsymbol{R}_e\right) cos\varphi_A - \left[\boldsymbol{R}_e^2 - \left(\boldsymbol{H} + \boldsymbol{R}_e\right)^2 \sin^2\varphi_A\right]^{1/2} , \tag{17}$$

where $\boldsymbol{V}_s$ is the ground velocity along the scanning direction generated by the orbital motion of the satellite, $\boldsymbol{V}_e$ is the tangential velocity caused by the spin motion of the earth, τ is the angular velocity of orbital precession, and ω_e is the rotational angular velocity of the earth.

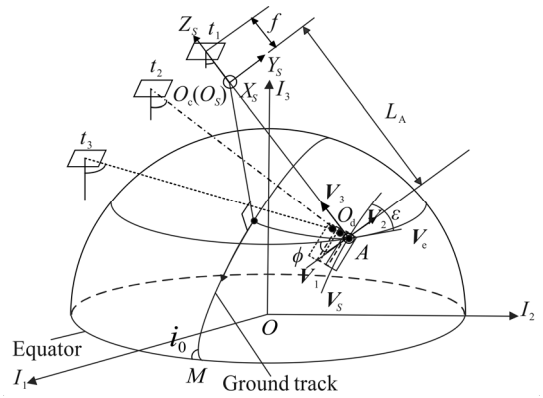

Fig.4 Equivalent circuit diagram with satellite lateral swing

In Fig.4, $\boldsymbol{V}_1$, $\boldsymbol{V}_2$, $\boldsymbol{V}_3$ and ε are

$$\boldsymbol{V}_1 = \boldsymbol{V}_s + \boldsymbol{V}_e \cos\varepsilon , \tag{18}$$

$$\boldsymbol{V}_2 = \boldsymbol{V}_e \sin\varepsilon , \tag{19}$$

$$\boldsymbol{V}_3 = \boldsymbol{V}_e \sin\varepsilon\cos\phi , \tag{20}$$

$$\varepsilon = \pi/2 - \angle MFG = \arcsin\left[\cos i_0 / \cos\left(\pi/2 - \lambda_A\right)\right], \tag{21}$$

$$\phi = \vartheta . \tag{22}$$

The relationship between the vector maps from the object coordinate system to the image plane coordinate system is

$$\boldsymbol{V}_p = \begin{bmatrix} V_{p1} \\ V_{p2} \\ V_{p3} \end{bmatrix} = \begin{bmatrix} -\frac{f}{L_A} & 0 & 0 \\ 0 & -\frac{f}{L_A} & 0 \\ 0 & 0 & 1 \end{bmatrix} \begin{bmatrix} V_1 \\ V_2 \\ V_3 \end{bmatrix} , \tag{23}$$

$$\psi_A = \arctan \frac{V_{p2}}{V_{p1}} . \tag{24}$$

Due to the high investment and risk, it is necessary to build a simulation system on the ground to test and verify the band splicing algorithm. As shown in Fig.5, the experimental system establishes the orbit model with PXI dynamic server. The attitude control system with sensitive part simulates the satellite platform maneuver. The time delayed and integration (TDI) charge coupled device (CCD) camera system is placed on the attitude control system platform. They work together to carry out the imaging of the P4 type LED earth dynamic screen. The attitude control system includes triaxial flotation turntable and attitude control groupwares composed of fiber optical gyro, tilt sensor, flywheel and data acquisition card, etc, as shown in Fig.6(a). Fig.6(b) shows the TDI CCD camera system, which consists of lens, light aperture and mirror components.

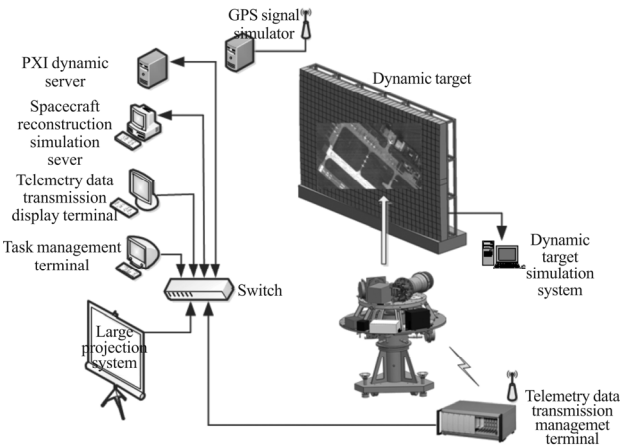

Fig.5 Schematic diagram of experimental setup

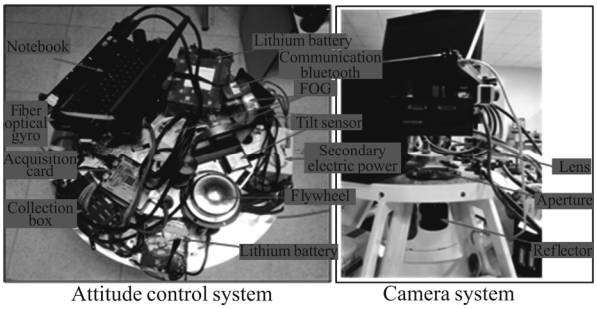

Fig.6 Composition of the experimental equipment

The curvature radius of the earth is 6 378 km. The orbit altitude is 500 km. The TDI CCD pixel size is 8.75 μm and its corresponding resolution is 0.625 m. The focal length of camera is 7 m. The moving speed of satellite relative to the ground is 7.3 km/s and the rotation speed of the earth is 370 m/s, the ratio of which is approximately 20:1.

The simulation parameters need to be selected according to the scaling principle on the ground. The curvature radius of P4 type LED dynamic screen is designed to be 32 m. The object distance is 2.5 m. The pixel size is 8.75 μm and its corresponding resolution is 4 mm. The camera focal length is 5.5 mm. The speed of target is 20 pixels per second. The simulation speed of the earth rotation is 1 pixel per second. Considering the ranges of the camera roll angle and the pitch angle, the LED large screen size is designed to be 5 m×3 m. The other specific parameters are shown in Tab.1.

It is necessary for satellite to be with high attitude control accuracy, rapid mobility, and high precision horizontal matching to ensure the band strict registration. The three-axis attitude angles of band starting points can be calculated through Eq.(13), Eq.(14) and Eq.(24). The attitude and imaging parameters are shown in Tab.2.

Tab.1 Scaling parameters

Original parameter	Value	Simulation parameter	Value
Earth radius	6 378 km	LED radius of curvature	32 m
Orbit altitude	500 km	Relative object distance	2.5 m
Camera focal length	7 m	Camera focal length	5.5 mm
Pixel size	8.75 μm	Pixel size	8.75 μm
Imaging resolution	0.625 m	Imaging resolution	4 mm
Roll angle range	±40°	Corresponding swath	4.2 m
Pitch angle range	±25°	Corresponding swath	2.3 m
Motion speed of satellite relative to ground	7.3 km/s	Target velocity in X direction	20 pixels per second
Earth rotation speed	370 m/s	Target velocity in Y direction	1 pixel per second

First of all, as shown in Fig.7, the dynamic target speed is adjusted to be 20 pixels per second along X axis and 1 pixel per second along Y axis. Secondly, take the center of screen as the benchmark and adjust the turntable alignment to the target A. Open the camera and the three-axis attitude angles are kept as (10°, 30°, 2.44°) respectively for 5 s. Thirdly, the turntable maneuvers to the target B in 20 s in accordance with the speed of 2°/s. And then maintain the attitude (9.53°, 0°, 2.82°) and carry out the imaging of the band2 for 5 s. Finally, the turntable maneuvers to the target C in 20 s. The attitude angles are (9.1°, −30°, 2.45°) respectively. The imaging process lasts for 5 s.

Tab.2 Imaging theoretic attitude, actual attitude and the deviation between them

	Theoretic roll angle (°)	Theoretic pitch angle (°)	Theoretic yaw angle (°)	Actual roll angle (°)	Actual pitch angle (°)	Actual yaw angle (°)	Roll angle deviation (°)	Pitch angle deviation (°)	Yaw angle deviation (°)
Band1	10	30	2.44	10.018	30.012	2.427	0.018	0.012	−0.013
Band2	9.53	0	2.82	9.515	0.011	2.804	−0.015	0.011	−0.016
Band3	9.1	−30	2.45	9.119	−30.014	2.468	0.019	−0.014	0.018

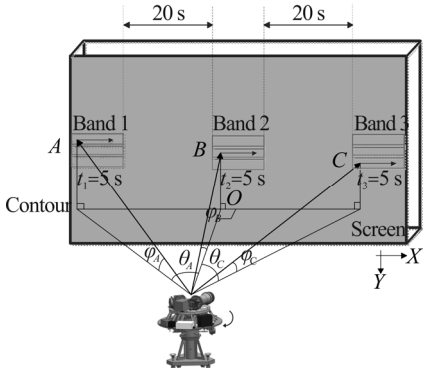

Fig.7 Process of simulation imaging

The imaging simulation is carried out on the emulational target and the scene image. There are three kinds of target shapes: single pixel, horizontal strip, and longitudinal strip. The result images are shown in Fig.8.

There is overlapping of 7 pixels and dislocation of one pixel between band1 and band2, whose overlapping rate is 10.93%. Between band2 and band3, there is overlapping of 5 pixels and dislocation of two pixels, whose overlapping rate is 9.09%. This warp has little effect on the imaging quality, which can be ignored.

In this paper, an attitude determination problem is analyzed based on the band splicing imaging principle of

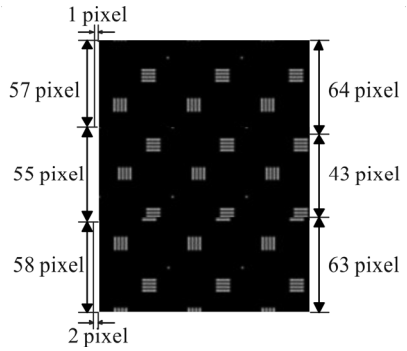

Fig.8 Sketch map of pixel overlap and dislocation

agile satellite. The image matching attitude algorithm for each strip is determined according to the matching relationship between the optimal tracking path and the direction of the thrust. Finally, the three-band geometric scaling experiment is carried out. The experimental results prove that the algorithm is accurate, and it can realize the matched band splicing imaging.

References

[1] F. J. Delgado, J. M. Quero, J. Garcia, C. L. Tarrida, P. R. Ortega and S. Bermejo, IEEE. Trans. Ind. Electron. **59**, 4871 (2012).

[2] Longbotham N, Bleiler C and Chaapel C, Spectral Classification of Worldview-2 Multi-angle Sequence, IEEE GRSS and ISPRS Joint Urban Remote Sensing Event. Munich: IEEE Computer Society, 109 (2011).

[3] T. Sun, F. Xing, Z. You and M. Wei, Opt. Express **21**, 20096 (2013).

[4] YU Jing, XI Jin-jun, YU Long-jiang and JIANG Fang-hua, Spacecraft Engineering **24**, 27 (2015). (in Chinese)

[5] ZHANG Xin-wei, DAI Jun and LIU Fu-qiang, Spacecraft Engineering **20**, 32 (2011). (in Chinese)

[6] W. Zhang, W. Quan and L. Guo, Sensors (Basel) **12**, 6712 (2012).

[7] HUANG Qun-dong, YANG Fang and ZHAO Jian, Spacecraft Engineering **22**, 17 (2013). (in Chinese)

[8] YANG Xiu-bin, JIANG Li and SU Chang, Acta Optica Sinica **32**, 0911004 (2012). (in Chinese)

[9] Wang Ya-min, Yang Xiu-bin, JIN Guang, Xu Wei and Zhang Zhao, Acta Photonica Sinica **46**, 0311002 (2017). (in Chinese)

[10] SUN Zhi-yuan, JIN Guang, ZHANG Liu, XU Kai and CHEN Mao-sheng, Infrared and Laser Engineering **19**, 2715 (2011). (in Chinese)

[11] M. S. Wei, F. Xing, B. Li and Z. You, Sensors (Basel) **11**, 9764 (2011).